Delamination fracture toughness of continuous glass-fiber/epoxy composites for structural applications

D. Treber, B. Haspel, P. Elsner, Kay A. Weidenmann

Angaben zur Veröffentlichung / Publication details:

Treber, D., B. Haspel, P. Elsner, and Kay A. Weidenmann. 2017. "Delamination fracture toughness of continuous glass-fiber/epoxy composites for structural applications." *International Journal of Plastics Technology* 21 (1): 39–54. https://doi.org/10.1007/s12588-016-9168-x.

Delamination fracture toughness of continuous glass-fiber/epoxy composites for structural applications

D. Treber[1] · B. Haspel[1] · P. Elsner[1] · K. A. Weidenmann[1]

Abstract This paper presents experimental results of delamination fracture toughness tests on glass-fiber/epoxy composites which are manufactured in a novel Compression Resin transfer molding (CRTM) process in comparison to the performance of a well-studied RTM reference process. The examined laminates are built out of six plies, with a plain weave fiber orientation. 90% of the fibers are in longitudinal direction and 10% are perpendicular woven in. The influence of the process regarding interlaminar fracture toughness is tested under pure mode I (DCB), pure mode II (ENF) and mixed mode loading (MMB). The aim of this study is to establish a semi-empirical criterion to derive the interlaminar fracture toughness of all mixed-mode ratios using the pure mode I or II loading fracture toughnesses. It has been found, that the materials performance for both processes are comparable, however the fracture behavior is strongly influenced by the fabric structure. The examination of the laminates polymer system showed a strong R-curve behavior for mode I and mode II loading. It was possible to establish a semi empirical criterion that shows good agreement with the experimental results.

Keywords RTM · Compression RTM · Mixed mode · Strain energy release rate

Introduction

Fiber-reinforced composites, which show steady growth rates in many technical areas, are very attractive for applications, where a high stiffness-to-weight and strength-to-weight ratio is needed. Due to a significant weakening of the composite

✉ K. A. Weidenmann
kay.weidenmann@kit.edu

[1] Institute for Applied Materials (IAM–WK), Karlsruhe Institute of Technology (KIT), Engelbert-Arnold-Straße 4, 76128 Karlsruhe, Germany

system through delamination that leads to a loss of stiffness, strength and expected service life, a precisely knowledge of the crack growth behavior is essential. To improve and to understand the materials performance not only knowledge regarding the macro mechanical damage behavior, but also the micro mechanical properties of the composites are indispensable.

In the literature extensive research has been done on determining the interlaminar fracture toughness of unidirectional laminates [1–3]. The interlaminar fracture toughness is commonly evaluated by applying the linear elastic fracture mechanics (LEFM). The most common failure mode for delamination is found to be mode I, mode II or mixed mode I + II. For determining pure mode I, Double cantilever beam (DCB) testing is commonly used [4–6], for pure mode II load the End notched flexure (ENF) test was prevalently chosen [7, 8]. In most realistic, near-service loading cases composite structures are subjected to both loading modes, therefore mixed-mode testing gives the most realistic results. Because of the advantages of the mixed mode bending (MMB) test, in comparison to other test configurations with mixed-mode loading which are proposed in the literature [9], and the fact that the MMB test combines the DCB and ENF tests, this configuration was chosen within the scope of this study.

The existence of a rising resistance curve (R-curve) was reported in many studies on unidirectional laminates [10–12]. The micromechanisms corresponding to this effect occur at the crack tip. Hashemi et al. [11, 13] reported that there are two main effects upon DCB-tests that lead to a R-curve behavior on unidirectional laminates, based upon thermoplastic-matrices composites: Firstly, the magnitude of fiber bridging increases as the crack grows. Secondly, the occurrence of subcritical cracks in front of the crack tip leads to crack tip splitting and further fiber bridging. For the ENF test, it was found by Hashemi et al. [11, 13], that the increase of the fracture toughness is caused by the increase of the size of the plastic damage zone around the crack tip as the delamination propagates. Another influence factor on ENF testing was reported by Carlson et al. [7], who documented that the friction between the crack surfaces above the fulcrum on crack initiation point increase the fracture toughness, because sliding of the crack surfaces is necessary for crack propagation.

The crack propagation for unidirectional laminates has been stable in deformation-controlled DCB-tests and unstable in deformation-controlled ENF-Test, where the initiation crack is shorter than 35% of the span length [8].

The materials used in this study have 10% of the fibers woven perpendicular, therefore studies which examined interlaminar fracture behavior on woven composites will here be presented as well. For plain weave thermosetting materials in DCB tests a “stick-slip” crack propagation behavior that is defined by stable crack growth interrupted by unstable jumps was observed and the existence of a R-curve through intensive fiber-bridging was documented [14, 15]. In the ENF tests a stable crack growth and intensive ply bridging and fiber branching occurred that lead, as reported in the DCB tests, to a R-curve behavior for fracture toughness under pure mode II loading [14].

The present study concerns interlaminar fracture testing of glass-fiber/epoxy composites manufactured by two different resin transfer molding (RTM)-processes, the classical RTM (RTM)-process [16] as reference process and the novel

Compression RTM (CRTM)-process [17], that is characterized by shorter cycle times and therefore allows a more economical manufacturing of efficient structural components. The main purpose of this study is to compare these two processes by delamination fracture toughness under various modes of loading and to establish a semi-empirical criterion [18] that shows good agreement with the experimental results with the purpose to clarify potential influences of the processing route on the material properties.

Experimental

The two fiber/epoxy composite panels used were prepared from six-ply plain weave E-glass fiber prepregs, from P-D Interglas Technologies AG, in which 90% of the fibers were in longitudinal direction of the specimens and 10% were perpendicularly woven in. This panels were manufactured by two different processes, the RTM- and the Compression-RTM-process. The epoxy resin system XB3585-XB3458 from the enterprise Huntsman International LLC was used in both processes. All specimen panels were manufactured at the facilities of the Fraunhofer Institute of Chemical Technology (ICT) in Pfinztal. The material characteristics are given in Table 1. To simulate the delamination, a 13 μm thin PTFE film was inserted at the mid-plane between the third and the fourth ply. From the panels, the test specimens for all the various mode loadings were cut to be nominally 20 mm wide and 120 mm long. The panels were 2 mm thick in average. The initial crack length caused by the PTFE film was around 40 mm. To apply the mode I- and mixed-mode-load, standard steel hinges (DIN 7954 form D with a height of 25 mm) were bonded onto the specimens with the two-components epoxy resin adhesive "UHU plus endfest 300". The hinges were glued onto the specimens in a way, that a starting crack length, from the end of the hinge to the initial start of the crack, of 24 mm was achieved. To attain good bonding the surface of the specimens and hinges were grit-blasted and cleaned with an acetone-impregnated cloth before the adhesive was applied and cured at a temperature of 125 °C for 15 min. During gluing, the hinges were clamped to the specimens in order to avoid slipping. The specimens were marked at one longitudinal edge with white paint to render the crack tip more visible. Due to the testing standards [19–21] a constant displacement rate of 4 mm/min was used for the mode I- and mixed-mode-loading, for the mode II-test a constant displacement rate of 2 mm/min was applied. A continuous load-displacement graph was recorded throughout the tests. Delamination was observed visually with a

Table 1 Measured material properties of the six-ply laminates from previous works

Characteristic value	E-glass-fiber	Huntsman XB 3585	RTM	CRTM	Unit
E_{11}	76.6	4.1	39.5	37.4	GPa
E_{22}	76.6	4.1	14.3	14.2	GPa
Fiber mass fraction (φ)	–	–	49.6	46.7	vol%
Shear modulus (G_{12})	30.4	1.5	2.9	2.7	GPa

digital microscope type VHX-600 from Keyence with a magnification of 50–100 times. For implementation of the tests a universal testing machine (type Zwick/Roell) with a maximum capacity of 2, 5 kN was used. To record the displacement for the DCB test the crosshead displacement of the testing machine was registered. An external displacement transducer was installed for the ENF and MMB tests to avoid any deterioration of the results due to the compliance of the machine. Due to the expected higher scattering eight specimens were tested for each of the two manufacturing processes in the DCB. Five specimens were tested for each loading condition and each manufacturing process in the MMB test and in the ENF test. To analyze the interlaminar fracture mechanisms the fracture surfaces of mode I and mode II specimens were examined in a scanning electron microscope (SEM).

DCB-test

To eliminate any influence of the incorporated PTFE release film the first measuring point for the starting delamination was 10 mm after the initial crack. The specimens were then loaded until a total crack length of about 60 mm was achieved. The calculation of the interlaminar fracture toughness for pure mode I-loading was based on the European Standard DIN EN 6033 [19].

ENF-test

Interlaminar fracture toughness for pure mode II-loading was determined by the European Standard DIN EN 6034 [20]. The critical load at delamination crack onset was recorded when there was a small load drop or a visually observed delamination or when the straight with a slope of 95% of the slope between 10 and 30 N was exceeded by the load-displacement trace. The criterion that occurred first on the load deflection curve was chosen for calculation.

MMB-test

For the MMB testing the ASTM Standard D6671/6671 M-06 was used [21]. Four different test configurations with variable G_{II}/G-ratio and depending on that variable lever arm lengths, were tested. Because the parameters a_0, χ and h, that are necessary for calculating the lever arm length c are specimen depending, average values were used. To avoid a misrepresentation of the results the compliance of the machine was calculated via calibration tests. The calibration specimen was made of steel with an elastic linear modulus of 210 GPa. It was 30 mm in width, 10 mm thick and 130 mm long. The required slope m_{cal} of the load-displacement trace was recorded between 50 and 300 N. The parameters of the various MMB-setups are given in Table 2.

The estimated value of total mixed mode fracture toughness G_c^{est}, was valued by Eq. (1) based on the results of the ENF and DCB tests.

$$G_c^{est} = \left(1 - \frac{G_{II}}{G}\right) G_{IC} + \frac{G_{II}}{G} G_{IIC} \tag{1}$$

Table 2 Parameters of the variable MMB test setups

G_{II}/G (%)	c (mm)	c_g (mm)	P_g (N)	C_{cal} (mm/N)	m_{cal} (N/mm)	C_{sys} (mm/N)
21	115.7	37.0	10.036	4.4×10^{-4}	767	8.7×10^{-4}
31	69.6	27.0	10.036	2.3×10^{-4}	838	9.7×10^{-4}
44	51.9	24.7	10.036	1.7×10^{-4}	1623	4.5×10^{-4}
69	33.4	17.4	10.036	1.1×10^{-4}	1945	4.0×10^{-4}

Table 3 Estimated values of total fracture toughness for the different G_{II}/G ratios

G_{II}/G (%)	RTM G_c^{est} (J/m^2)	CRTM G_c^{est} (J/m^2)
21	555	575
31	631	645
44	729	736
69	917	912

The estimated values of total mixed mode fracture toughness are given in Table 3.

The tests were performed with a pre-load of 5 N prior to recording the load-displacement graph. After reaching the last marker or the maximum measurable displacement of 20 mm, the specimen was relieved with a constant displacement rate of 20 mm/min.

Results

The different results for the strain energy release rate obtained in MMB tests via ASTM Standard D6671/D6671M-06 are considerably varying as shown in Fig. 1. The values reported are in good agreement with the ASTM Standard, in which a trend line is recorded for unidirectional reinforced composites. The values determined with the "5%/max" criterion overestimate the fracture resistance, while the best results were gained with the visual detection (VIS). These values showed the lowest scatter. Therefore for fracture toughness investigations under mixed mode loading only the values determined through the VIS-criterion are considered.

The results show a comprehensible trend: The higher the G_{II}/G modal ratio, the greater is the value of fracture toughness. In Fig. 2 the interlaminar fracture toughness of mode I and II, G_I and G_{II} are displayed versus the mode II ratio. In the higher mode II ratio range G_{II} increases disproportionately, while G_I increases less in the mode I dominant range and even stays constant from a mode II ratio of 25% till 0%. Because the total fracture toughness G_C in MMB test is the summation of both pure mode loading fracture toughnesses, the rise of the total fracture toughness G_C with increasing mode II ratio is disproportionately in the range where the mode

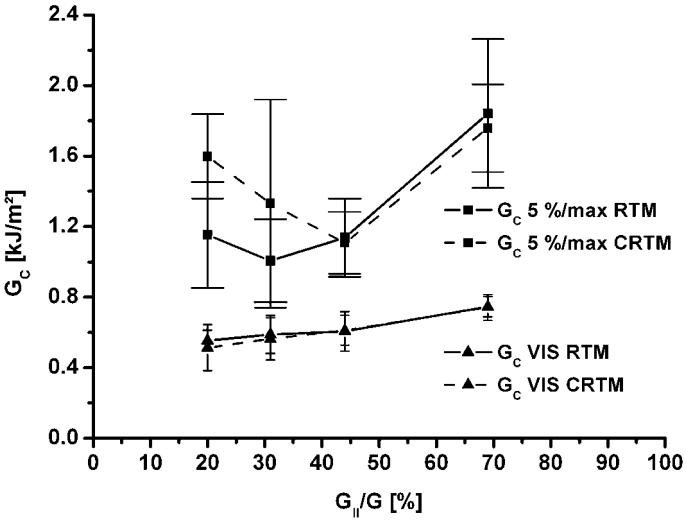

Fig. 1 MMB results of the "5%/max" and "VIS" criterion for the total fracture toughness G_C obtained via the ASTM Standard D6671/D6671M-06 displayed versus the mode II ratio

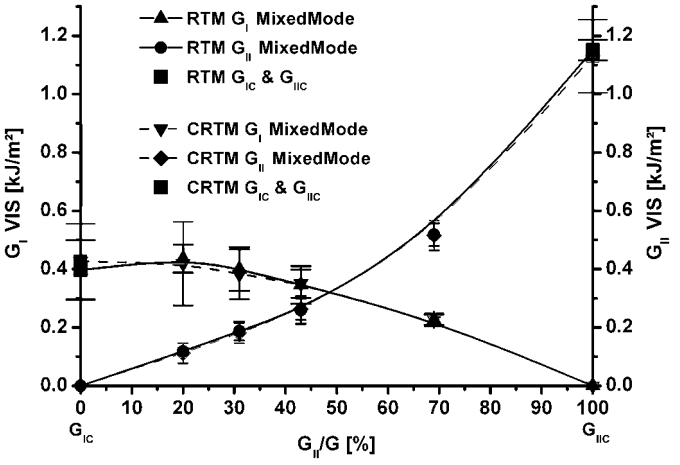

Fig. 2 G_I and G_{II} versus mode II ratio

II loading is dominant, as can be seen in Fig. 3. This disproportionate increase gets traced back to increasing multiple fracture of the brittle matrix between the fibers with increasing shear loading [22].

The load-displacement plots of the DCB tests revealed crack propagation with unstable jumps of type shown in Fig. 4. This "stick-slip" propagation behavior was already reported elsewhere [23, 24] and clearly impedes determining fracture resistance, which can be seen on the large scatter of the results for the DCB test. The causes of this partially unstable behavior are discussed later in this contribution. The determination of the fracture toughness for mode I loading via the "area" method,

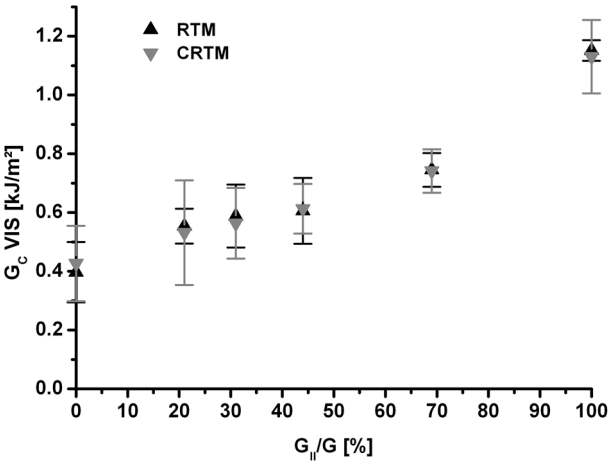

Fig. 3 Total fracture toughness G_C versus mode II ratio

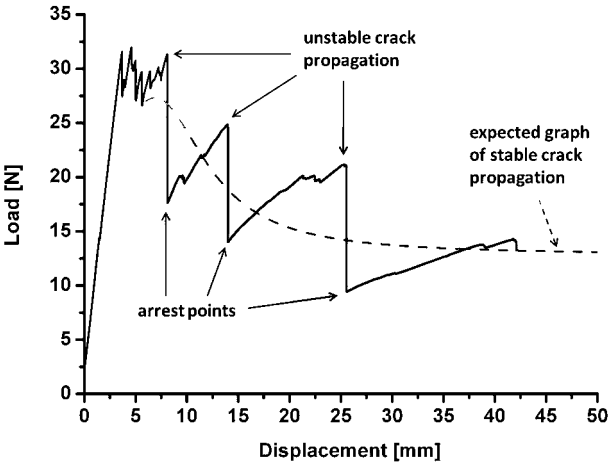

Fig. 4 Mode I load-displacement plot, "stick-slap" crack growth behavior

used in the European standard DIN EN ISO 6033 [19], leads to an average fracture toughness over some value of crack propagation [11]. Therefore the error created by unstable crack growth interruptions gets reduced, but fracture toughness is significantly depending on crack length [23].

The ENF test showed stable crack initiation, that is caused by a larger increase of the fracture toughness through fiber bridging and ply branching than the decrease of the strain energy release rate with crack length [14].

Stable Propagation in the mixed mode bending test increased with increasing mode II ratio.

In DCB tests extensive fiber bridging and crack jumping from one ply to another by both processes was observed. Figure 5 shows the fiber bridging effect at a CRTM

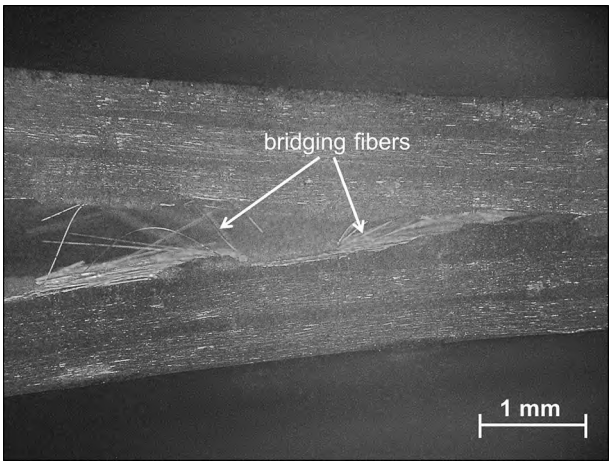

Fig. 5 Fiber bridging at mode I loading

specimen under mode I loading. This effect and the fact that subcritical cracks occurred in front of the crack tip lead to the documented resistance curves (R-curve) for G_{IC} in MMB tests displayed in Fig. 6 [11, 13]. The recording of R-curves was only possible in the MMB test as several measuring points have been recorded. The application of the European Standards DIN-EN 6033 and DIN-EN 6034 for the DCB and ENF test and the resulting test implementations prevented determining an R-curve for these loading conditions. It can be seen that the increase of fracture toughness with crack length is much larger with a low mode II ratio. With higher mode II ratios the fracture toughness curves flatten out. The 69% mode II ratio configuration even reaches a plateau from around 34 mm of crack length, where no further increase of fracture toughness is observed.

The rise of G_{IIC} with crack propagation (see Fig. 7) is due to an increase of the size of the plastic damage zone around the crack tip and intensive fiber bridging [11, 13, 14]. All mode II ratios except the 69% configuration show identical increase rates for the fracture toughness under mode II loading G_{IIC}. The 69% mode II ratio curve is steeper in the first range of crack growth and subsequently reaches as already seen for G_{IC} (see Fig. 6) a plateau from a crack length of around 34 mm.

The reason for the large scatter of the R-curves after the first two measuring points is documented by Reeder [25], who determined a limit of maximum displacement to keep the geometric nonlinear error below 5%. This criterion was violated by all mixed mode configurations.

Discussion

The experimental results show no significant difference between the values of fracture toughness of the two processes in the entire different mode II ratios; they vary in the same range. This is because the fracture behavior is dominated by the polymer system which was identical for both manufacturing processes [26]. The slightly higher fiber

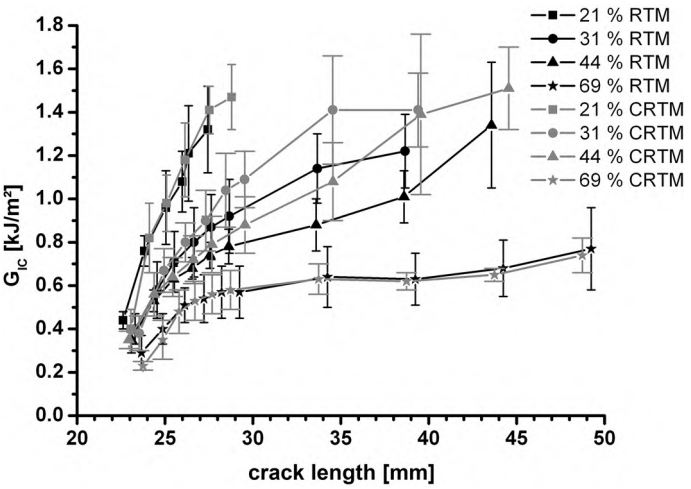

Fig. 6 R-curves in MMB tests for G_{IC} for different mode II ratios

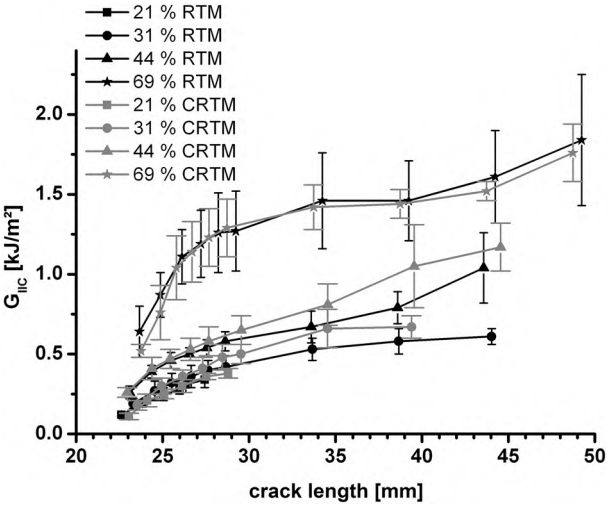

Fig. 7 R-curves in MMB test for G_{IIC} for different mode II ratios

mass fraction of the reference RTM process does not influence the fracture toughness, neither do the manufacturing discrepancies. Therefore no distinction between the two processes will be made in the following chapter and the fractographic analysis will clarify the fracture behavior of the polymer system used for both processes.

Fractographic analysis

The fractographic analysis showed as already declared no difference between the two examined processes.

SEM examination of the pure mode I specimens showed large areas of clean fracture surface, where the crack grew through the resin (see Fig. 8). The adhesion between the fibers and the matrix was accordingly partially better than the cohesion inside the resin matrix. Unstable crack jumps offered different damage symptoms: In the first millimeters of the unstable crack growth, the crack propagated along the resin fiber interface (see Fig. 9). Hine et al. [27] reported for PEEK/carbon fiber composites that unstable crack propagation is caused by areas of higher fracture toughness. If the crack reaches a region of higher fracture toughness, the propagation stagnates until there is enough saved elastic energy for further crack propagation. After passing the region of higher fracture toughness, there is still excess energy that keeps the crack propagating unstable. Indeed, investigations carried out by Hine et al. included a temperature change to alter the matrix ductility in a controlled way. This was not the case for the investigations presented here with an epoxy matrix investigated at constant room temperature whose toughness may not alter. Therefore, it is much more likely, that the change in crack propagation stability is due to the local fiber architecture. Following the results found by Kotaki et al. [28] perpendicular woven in fiber skeins may represent higher fracture toughness areas. This phenomenon is observed here and displayed in Fig. 9. The crack propagated stable in-between the resin and after the perpendicular woven in skein unstable along the fiber resin interface, which may be because there was enough energy to break up the interface bindings. As soon as the excess of elastic energy was reduced, the crack development grew still in an unstable manner but again in-between the resin area. To explain this change of failure mechanism while unstable crack growth, further examinations of the interface properties of the used polymer system have to be done. Indeed, the authors have shown in preliminary investigations based on push-out tests, that the fiber-matrix interface features an interfacial strength of 80 MPa indicating an excellent bonding [29]. This coincides

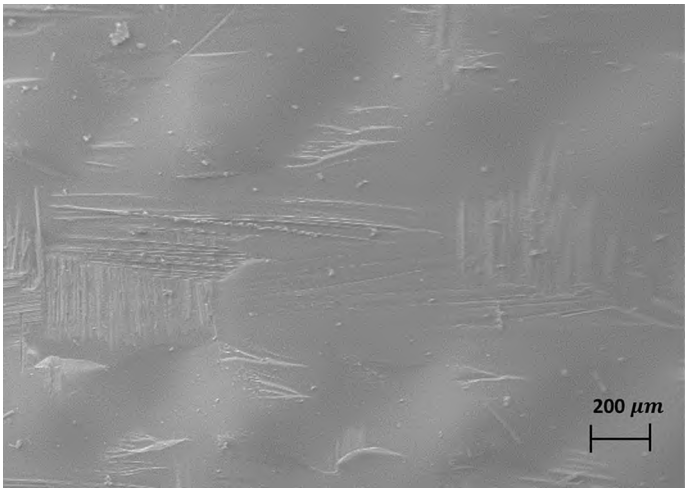

Fig. 8 Large areas of clean fracture surface, crack growth through the resin

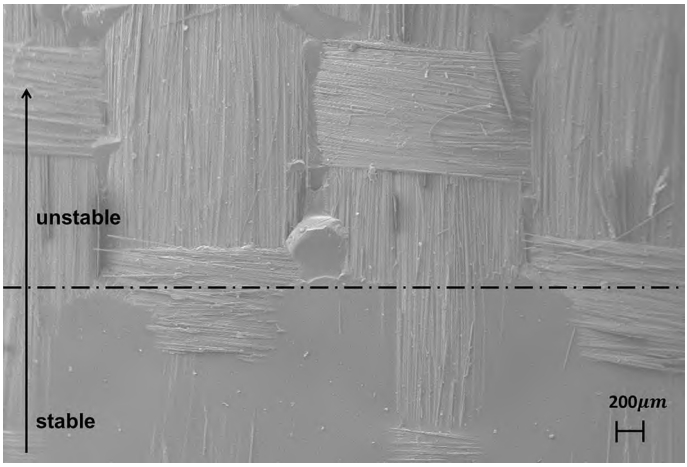

Fig. 9 Transition area of stable propagation to unstable propagation

with the results presented by Kotaki et al. showing that an increase of fiber-matrix bonding enhanced by adding coupling agent results in a change from continuously stable to a mix of stable and unstable crack propagation. Consequently, the observation of a crack propagation as given in Fig. 4 is correlated to a good fiber matrix bonding.

The specimens under pure mode II loading showed completely different fracture surfaces. It was observed, that the shear mode leads to multiple fracture in brittle matrix systems as can be seen in Fig. 10, that leads to the much higher fracture toughness for pure mode II loading, because a much higher volume of polymer has to be fractured [22]. The matrix shows a shear loading typical hackle–type of fracture. The fibers get crushed into many chunks as well as shown in the dashed rectangle. A pronounced fiber-bridging effect was visible, too (see Fig. 11). This effect also increases the determined fracture toughness G_{IIC} as reported by [30]. The glass fibers pulled out show shear hackles typical for shear loading attached to them [22]. This is another indicator of the good fiber matrix interface of the specimens' resin system.

Application of a semi-empirical failure criterion

Based on the specimen material and knowledge of the fracture mechanisms generated by the SEM analysis, a semi-empirical failure criterion shall be introduced. For epoxy resin laminates reinforced with E-glass fibers Benzeggagh and Kenane [10] suggest the following relationship:

$$G_C = G_{IC} + (G_{IIC} - G_{IC})\left(\frac{G_{II}}{G}\right)^{m_c} \tag{2}$$

In their study 95% of the fibers are in longitudinal direction and 5% of the fibers are woven perpendicularly. The parameter m_c which is required for this approach

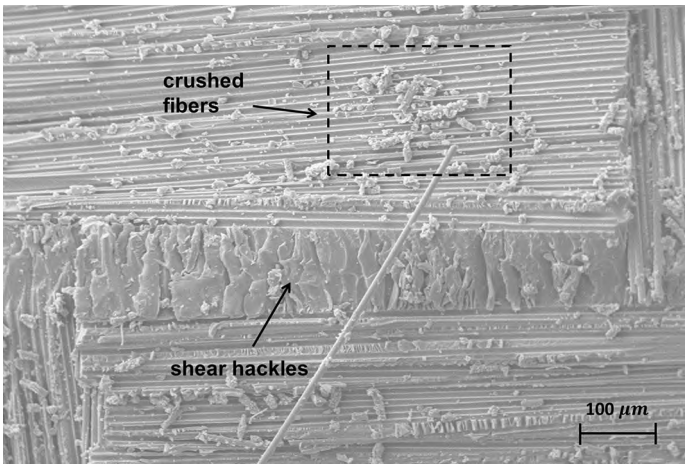

Fig. 10 Fracture surface after pure mode II loading: multiple fracture of the resin (array); chunks of crashed glass fibers (*dashed rectangle*)

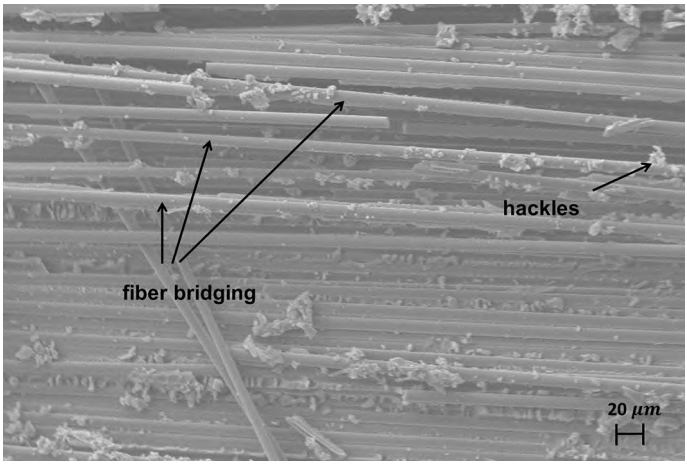

Fig. 11 Strong fiberbridging effekt after mode II loading; shear hackles on the pulled out glass fibers

was determined numerical with the method of least squares [31]. G_{IC} and G_{IIC} are the interlaminar fracture toughness values determined in the pure mode load tests. The calculated graphs as well as the experimental values for both processes are shown in Fig. 12. The calculated values are in good agreement with the experimental results for both processes. To investigate the possibility to gain results in mixed mode loading with just the pure mode loading tests, the parameter m_c was selected from literature [10], in which similar testing materials were used and analogical fracture mechanisms were observed. The results of this approach are displayed in Fig. 13. The results underestimate the total fracture toughness but can be used as a first approach for the materials investigated here

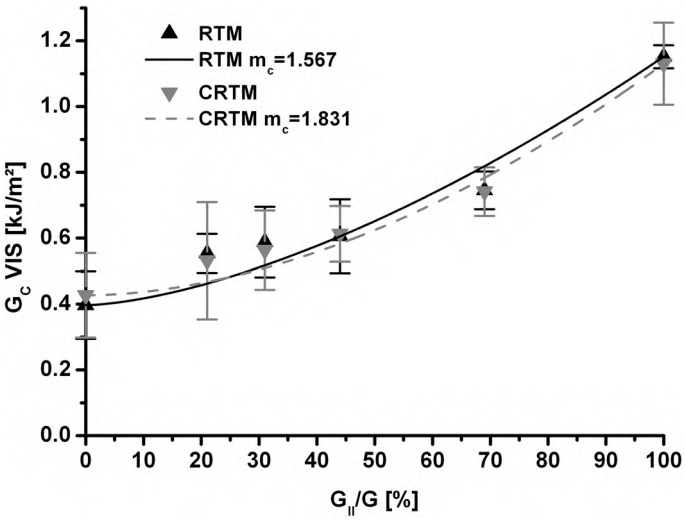

Fig. 12 Application of the semi-empirical criterion; determining mixed-mode values with the pure mode loading fracture toughnesses

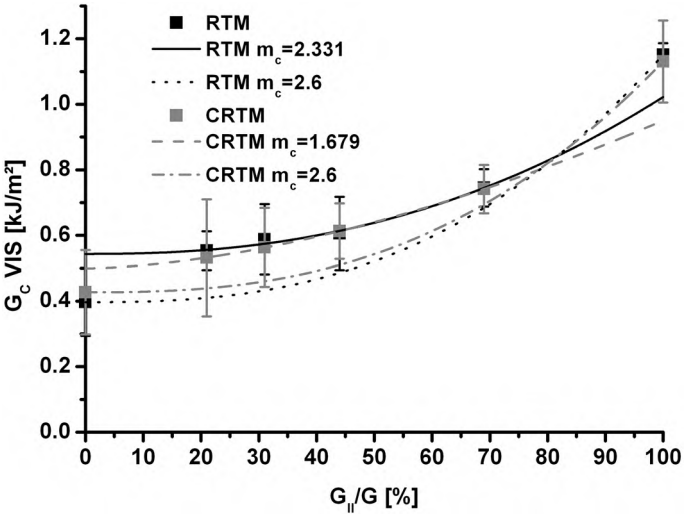

Fig. 13 Different approaches of the semi-empirical criterion: mc value from literature; determinig the pure mode fracture toughnesses via the mixed mode results

A contrary contemplation of the mentioned relationship (Eq. 2) shows that an extrapolation of the pure mode fracture toughness out of the mixed mode values are possible. For this purpose a system of linear equations consisting of the values of the four different mode II ratios was prepared. Because of three variables among four equations, the results of the configuration with a mode II ratio of 44% were neglected. The results are shown in Fig. 13 via the dashed lines. The value for G_{IC}

gets overestimated but is still in the range of scatter for both processes. In contrary the fracture toughness for pure mode II loading is underestimated. The agreement of experimental results end extrapolated values is reasonable but not as good as for the contrary contemplations.

Summary and conclusion

The main purpose of this study was to evaluate the interlaminar fracture properties of specimens manufactured with a new process, the CRTM-process in comparison to a well-studied reference RTM process. The second aim was to examine the application of a semi empirical criterion.

The CRTM specimen show identical results and inferior the reference RTM-process in no way. Although 90% of the fibers are unidirectional and only 10% are woven in perpendicular, the damage behavior was strongly influenced by the transverse skeins. A stick-slip crack growth behavior was observed in DCB tests and stable crack propagation occurred under pure mode II loading. The ENF test revealed a strong fiber bridging effect.

The MMB tests revealed a R-curve behavior for G_{IC}, that is caused by a strong fiber-bridging and subcritical cracks in front of the crack tip. Crack jumping with ply changes lead to further fiber bridging. G_{IIC} increased as well with increasing crack propagation. The SEM examinations showed here even more intensive fiber bridging and multiple fracture of the matrix resin is present, the evoked fracture resistance is much higher than under pure mode I loading.

Good Agreement was found between the experimental determined results and the values gained by application of the semi empirical criterion. The parameter m_c was determined through the method of least squares. For the reference RTM process good agreement was achieved with $m_c = 1.567$ and with $m_c = 1.831$ a good approximation for the CRTM process was achieved. In a different approach, a value for m_c was chosen from literature and applied to the pure mode loading results. It was found that this approach underestimates the fracture toughness, but is still good enough for a first approximation. In a contrary utilization of the criterion, the gained mixed mode results were used to obtain the pure mode loading fracture toughnesses. A reasonable agreement between the experimental results and extrapolated values for this contemplation has been found.

Acknowledgements The authors gratefully acknowledge Dr. Raman Chaudhari for the manufacture of the RTM panels at the Fraunhofer ICT. They also appreciate the financial support from the KITe hyLITE innovation cluster funded by the Fraunhofer Gesellschaft, the Karlsruhe Institute of Technology and the state of Baden-Württemberg.

References

1. Friedrich K (ed) (1989) Application of fracture mechanics to composite materials. Elsevier Science Publishers B.V, Amsterdam
2. Sela N, Ishai O (1989) Interlaminar fracture toughness and toughening of laminated composite materials: a review. Composites 20(5):423–435

3. Davies P, Blackman BRK, Brunner AJ (1998) Standard test methods for delamination resistance of composite materials: current status. Appl Compos Mater 5(6):345–364
4. Whitney JM, Browning CE, Hoogsteden W (1982) A double cantilever beam test for characterizing Mode I delamination of composite materials. J Reinf Plast Compos 1(4):297–313
5. Hashemi S, Kinloch AJ, Williams JG (1989) Corrections needed in double- cantilever beam tests for assessing the interlaminar failure of fibre composites. J Mater Sci Lett 8(2):125–129
6. Davies P, Benzeggagh ML (1989) Interlaminar Mode-I fracture testing. In: Friedrich K (ed) Application of fracture mechanics to composite materials. Elsevier Science Publisher B.V, Amsterdam, pp 81–112
7. Carlsson LA, Gillespie JW Jr, Pipes RB (1986) On the analysis and design of the end notched flexure (ENF) specimen for Mode II testing. J Compos Mater 20(6):594–604
8. Carlsson LA, Gillespie JW Jr (1989) Mode-II interlaminar fracture of composites. In: Friedrich K (ed) Application of fracture mechanics to composite materials. Elsevier Science Publisher B.V, Amsterdam, pp 113–157
9. Reeder JR, Crews JRJ (1990) Mixed- mode bending method for delamination testing. AIAA J 28(7):1270–1276
10. Benzeggagh ML, Kenane M (1996) Measurement of mixed-mode delamination fracture toughness of unidirectional glass/epoxy composites with mixed-mode bending apparatus. Compos Sci Technol 56(4):439–449
11. Hashemi S, Kinloch AJ, Williams JG (1990) Mechanics and mechanisms of delamination in a poly(ether sulphone)- fibre composite. Compos Sci Technol 37(4):429–462
12. Szekrenyes A, Uj J (2005) Mode-II fracture in E-glass-polyester composite. Compos Mater 39(19):1747–1768
13. Hashemi S, Kinloch AJ, Williams JG (1990) The effects of geometry, rate and temperature on the Mode I, Mode II and mixed-Mode I/II interlaminar fracture of carbon- fibre/poly(ether-ether ketone) composites. J Compos Mater 24(9):918–956
14. Martin RH (1997) Delamination characterization of woven glass/polyester composites. J Compos Technol Res 19(1):20–28
15. Alif N, Carlsson LA, Gillespie JWJ (1997) Mode I, Mode II, and mixed mode interlaminar fracture of woven fabric carbon/epoxy. In: Hopper SJ (ed) Composite materials: testing and design, thirteenth volume, ASTM STP 1242, 13th edn. American Society for Testing and Materials, West Conhocken, pp 82–106
16. Potter K (1997) Resin transfer moulding. Chapman & Hall, London
17. Young W-B, Chiu C-W (1995) Study on compression transfer molding. J Compos Mater 29(16):2180–2191
18. Gong X-J, Benzeggagh M (1995) Mixed mode interlaminar fracture toughness of unidirectional glass/epoxy composite. In: Martin RH (ed) Composite materials: fatigue and fracture—fifth volume, ASTM STP 1230. American Society for Testing and Materials, Philadelphia, pp 100–123
19. DIN EN 6033 (1996) Determination of interlaminar fracture toughness energy-Mode I-GIC. Beuth-Verlag, Berlin
20. DIN EN 6034 (1996) Determination of interlaminar fracture toughness energy-Mode II-GIIC. Beuth-Verlag, Berlin
21. ASTM D 6671/D 6671M-06 (2006) Standard test method for mixed Mode I-Mode II interlaminar fracture toughness of unidirectional fiber reinforced polymer matrix composites. American Society for Testing and Materials, Philadelphia
22. Friedrich K (1989) Fractographic analysis of polymer composites. In: Friedrich K (ed) Application of fracture mechanics to composite materials. Elsevier Science Publisher B.V, Amsterdam, pp 425–487
23. Davies P, Moore DR (1990) Glass/Nylon-6.6 composites: delamination resistance testing. Compo Sci Technol 38(3):211–227
24. Starke C, Beckert W, Lauke B (1996) Characterization of the delamination behaviour of composites under mode I- and mode II-loading. Mater Sci Eng Technol 27(2):80–89
25. Reeder JR (2003) A criterion to control nonlinear error in the mixed-mode bending test. In: Bakis CE (ed) Composite materials: testing and design fourteenth volume, ASTM STP 1436. ASTM International, West Conshohocken, pp 349–371
26. Bradley WL (1989) Relationship of matrix toughness to interlaminar fracture toughness. In: Friedrich K (ed) Application of fracture mechanics to composite materials. Elsevier Science Publisher B.V, Amsterdam, pp 159–187

27. Hine PJ, Brew B, Duckett RA, Ward IM (1989) Failure mechanisms in continuous carbon-fibre reinforced PEEK composites. Compos Sci Technol 35(1):31–51
28. Kotaki M, Hamada H (1997) Effect of interfacial properties and weave structure on mode I interlaminar fracture behaviour of glass satin woven fabric composites. Compos A Appl Sci Manuf 28(3):257–266
29. Haspel B, Hoffmann C, Elsner P, Weidenmann K (2015) Characterization of the interfacial shear strength of glass-fiber reinforced polymers made from novel RTM processes. Int J Plast Technol 19(1):333–346
30. Alif N, Carlsson LA, Boogh L (1998) The effect of weave pattern and crack propagation direction on mode I delamination resistance of woven glass and carbon composites. Compos B Eng 29(5):603–611
31. Björk Å (1996) Numerical methods for least squares problems. Society for Industrial and Applied Mathematics, Philadelphia